Functional Characterization of Human Organic Anion Transporting Polypeptide B (OATP-B) in Comparison with Liver-Specific OATP-C

Ikumi Tamai,[1,2] Takashi Nozawa,[1] Minako Koshida,[1] Jun-ichi Nezu,[3] Yoshimichi Sai,[1,2] and Akira Tsuji[1,2,4]

Received April 21, 2001; accepted May 24, 2001

Purpose. To assess the functional characteristics of human organic anion transporter B (OATP-B) in comparison with those of the known, liver-specific OATP-C.

Methods. OATP-B or -C was expressed in HEK293 cells or *Xenopus* oocytes, and uptakes of estradiol-17β-glucuronide and estrone-3-sulfate were measured using radiolabeled compounds.

Results. OATP-C transported both estrone-3-sulfate and estradiol-17β-glucuronide, whereas OATP-B transported only the former. OATP-C-mediated uptake of estrone-3-sulfate exhibited biphasic saturation kinetics, whereas transports of estradiol-17β-glucuronide by OATP-C and estrone-3-sulafte by OATP-B followed single-saturation kinetics. Inhibition kinetics showed that only the high-affinity site for estrone-3-sulfate on OATP-C was shared with glucuronide conjugates. Uptake of [^{3}H]estrone-3-sulfate by OATP-B was inhibited by sulfate conjugates but not by glucuronide conjugates, whereas its uptake by OATP-C was inhibited by both types of conjugates.

Conclusions. OATP-B accepted sulfate conjugates of steroids but not glucuronide conjugates, whereas OATP-C transported both types of steroid conjugates. Transport of estrone-3-sulfate by OATP-B and -C followed single- and biphasic-saturation kinetics, respectively, and the high-affinity site on OATP-C was the same as that for estradiol-17β-glucuronide. Other OATPs, OATP-A and OATP-8, reportedly exhibit different preferences for steroid conjugates, and the specific recognition of sulfate conjugates seems to be unique to OATP-B.

KEY WORDS: organic anion; transporter; OATP; estrogen conjugates; liver.

INTRODUCTION

Numerous endogenous and xenobiotic organic anions are distributed to various tissues in the body and are eliminated mainly via the liver and kidney. Membrane transporters are involved in their efficient transfer between intra- and extracellular spaces. Various multispecific organic anion transporters, i.e., multidrug resistance-associated proteins (MRPs), organic anion transporters (OATs), organic anion transporting polypeptides (OATPs), and type I-inorganic phosphate transporter (NPT1), have been shown to be involved in these processes, playing physiologic roles as evidenced by their differential tissue distributions and subcellular localizations (1–4). Among them, rat oatp was molecularly identified as the first sodium-independent hepatic transporter (5). It is expressed in basolateral membranes of liver and is presumed to take part in the hepatic elimination of various anionic compounds (6). Homologous transporters have been cloned from mouse, rat, and humans, and their physiologic roles have been identified partially based on the functional and tissue distribution characteristics. In human, the OATP family is assigned the gene symbol SLC21A and includes prostaglandin transporter (PGT) (7), liver-specific transporter (LST) (8), and other OATP members (9–12). Among them, OATP-A (SLC21A3) and OATP-C (LST-1, OATP2, SLC21A6) are predominantly expressed in brain and liver, respectively, and are expected to have physiologic roles in brain distribution and/or efflux and hepatic elimination of anionic compounds, respectively (8–10). Although tissue expression profiles of seven members of human OATPs have been reported, the functional differences among these transporters are not clearly understood (7–9,11,12). Various organic anions could be transported by human OATPs and among them, conjugated metabolites of steroids such as estrone-3-sulfate and/or estradiol-17β-glucuronide are likely common substrates of human OATPs.

We showed that OATP-B (SLC21A9), -D (SLC21A11), and -E (SLC21A12) as well as OATP-C have differential characteristics regarding transport function and tissue distribution, but no precise studies have been done (12). Hepatic basolateral membrane-specific OATP-C has a broad substrate specificity, transporting conjugated metabolites of steroids, bile acids, prostaglandin, leukotriene, thyroid hormones, pravastatin, bilirubin and its conjugated metabolite, and benzylpenicillin, whereas OATP-B has shown negligible transport of estradiol-17β-glucuronide in comparison with estrone-3-sulfate, suggesting a distinct substrate specificity from that of OATP-C (8,10–13). In addition, because the tissue distribution of OATP-B is much broader than that of liver-specific OATP-C (12), OATP-B, and OATP-C are expected to have distinct functional roles.

Because so many OATP family members are present in humans, it is essential to characterize their differences in functional properties. For the better understanding of the role of each molecule, identifying the counterparts in animals is useful. However, in rats, for example, oatp-1 (5), -2 (14), and -3 (15), lst1 (oatp4) (16), and moat1 (17) are known, and additional transporters may exist. So, without precise functional analysis, it will be difficult to identify corresponding transporters in humans and animals. Accordingly, in the present study, the functional characterization of OATP-B was carried out in comparison with the better-understood OATP-C.

MATERIALS AND METHODS

Materials

[^{3}H]Estrone-3-sulfate, ammonium salt (1961 GBq/mmol), and [^{3}H]estradiol-17β-D-glucuronide (2035 GBq/mmol) were purchased from NEN Life Science Products, Inc. (Boston, MA). pcDNA3 Vector was obtained from Invitro-

[1] Faculty of Pharmaceutical Sciences, Kanazawa University, Kanazawa 920-0934, Japan.
[2] CREST, Japan Science and Technology Corporation, Kawaguchi 332-0012, Japan.
[3] Chugai Research Institute for Molecular Medicine Inc., Ibaraki 300-4101, Japan.
[4] To whom correspondence should be addressed. (e-mail: tsuji@kenroku.kanazawa-u.ac.jp)

0724-8741/01/0900-1262$19.50/0

gen (Carlsbad, CA). All other reagents for functional studies were purchased from Sigma Chemicals (St. Louis, MO) and Wako Pure Chemical Industries (Osaka, Japan).

Transport Experiments

For the transport experiments using HEK293 cells, the constructs pcDNA3/OATP-B and -C were used to transfect HEK293 according to the calcium phosphate precipitation method. HEK293 cells were routinely grown in Dulbecco's modified Eagle's medium containing 10% fetal calf serum, penicillin, and streptomycin in a humidified incubator at 37°C and 5% CO_2. After 24 h cultivation of HEK293 cells in 15-cm dishes, pcDNA/OATP or pcDNA vector alone was transfected by adding 20 μg of the plasmid DNA per dish. At 48 h after transfection, the cells were harvested and suspended in transport medium containing 125 mM NaCl, 4.8 mM KCl, 5.6 mM D-glucose, 1.2 mM $CaCl_2$, 1.2 mM KH_2PO_4, 1.2 mM $MgSO_4$, and 25 mM HEPES, adjusted to pH 7.4. The cell suspension and a solution containing a radiolabeled compound in the transport medium were separately incubated at 37°C for 20 min, then transport was initiated by mixing them. At appropriate times, 200-μL aliquots of the mixture were withdrawn and the cells were separated from the transport medium by centrifugal filtration through a layer of a mixture of silicone oil (SH550, Toray Dow Corning Co., Tokyo) and liquid paraffin (Wako Pure Chemical Industries) with a density of 1.03. Each cell pellet was solubilized in 3 N KOH and neutralized with HCl. Then, the associated radioactivity was measured by means of a liquid scintillation counter using cleasol-1 as a liquid scintillation fluid (Nacalai tesque, Kyoto, Japan). HEK293 cells transfected with pcDNA3 vector alone were used to obtain the background activity (termed mock).

Transport experiments by *Xenopus laevis* oocytes that were microinjected with *in vitro* synthesized complementary RNA (cRNA) of OATP-C using T7 RNA polymerase were performed by the method described previously (18). Briefly, defoliculated oocytes were injected with 50 nL of water containing 5 ng of cRNA, cultured for 2 days in modified Barth's solution (88 mM NaCl, 1 mM KCl_2 2.4 mM $NaHCO_3$, 0.82 mM $MgSO_4$, 0.33 mM $Ca(NO_3)_2$, 0.41 mM $CaCl_2$, and 10 mM HEPES adjusted to pH 7.4 with NaOH) and used for uptake experiments. Uptake of radiolabeled test compound was measured over 60 min at 25°C in the uptake medium (96 mM NaCl, 2 mM KCl, 1.8 mM $CaCl_2$, 1 mM $MgCl_2$, and 10 mM HEPES adjusted to pH 7.4 with NaOH), and the oocytes were solubilized in 5% SDS solution and the associated radioactivity was measured by liquid scintillation counter. As the control, the same volume of water was injected into oocytes and the uptake was measured in the same manner.

Reverse Transcriptase-Polymerase Chain Reaction (RT-PCR)

Expression of OATP-B and OATP-C in HEK293 cells transfected with cDNA of each transporter was confirmed by RT-PCR method. The specific primer pairs for OATP-B and OATP-C were 5′-CGTGCGGCCAAGTGTGTTCCATAA-3′ for forward and 5′-GAAGGAGTAGCCCCATAGC-CAATC-3′ for reverse and 5′-TGTCATTGTCCTTTT-AC-CTATTAT-3′ for forward and 5′-TGTAAGTTATTCCAT-TGTTTCCAC-3′ for reverse, respectively. The PCR reaction was preformed using SuperScript ONE-STEP™ RT-PCR System (GIBCO BRL, Rockville, MD) as follows: For OATP-B, the reaction was performed with 34 cycles of 94°C for 30 s, 55°C for 30 s, 72°C for 2 min, and final elongation of 72°C for 10 min. For OATP-C, it was 34 cycles of 94°C/30 s, 50°C/30 s, 72°C/2 min, and a final elongation of 72°C/10 min.

Analytical Methods

Cellular protein content was determined according to the method of Bradford by using a BioRad (Hercules, CA) protein assay kit with bovine serum albumin as the standard (19). Usually, initial uptake rates were obtained by measuring the uptake at 30 min. To estimate kinetic parameters for saturable transport, the uptake rate (v) was fitted to the following equations by means of nonlinear least-squares regression analysis using WinNonlin (Scientific Consulting Inc., Cary, NC).

In the case of a single saturable component,

$$v = V_{max}*s/(K_m + s)$$

and for a system consisting of two saturable components,

$$v = V_{max1}*s/(K_{m1} + s) + V_{max2}*s/(K_{m2} + s)$$

where v and s are the uptake rate and concentration of substrate, respectively, and K_m and V_{max} represent the half-saturation concentration (Michaelis constant) and the maximum transport rate, respectively. The uptake activity of OATP-B or -C by HEK293 cells was evaluated after subtracting the uptake by mock-transfected cells from total uptake by the OATP-B or -C-expressing cells. In the study using *Xenopus* oocytes, uptake of test compound by OATP-C was evaluated after subtracting the uptake by water-injected oocytes from the uptake by OATP-C cRNA-injected oocytes. All data were expressed as means ± SEM, and statistical analysis was performed by using Student's *t* test. Cell-to-medium ratio was obtained by dividing the uptake amount by the concentration of test compound in the uptake medium. The criterion of significance was taken to be $P < 0.05$.

RESULTS

Kinetic Analysis of Transport of Estrone-3-Sulfate and Estradiol-17β-Glucuronide by OATP-B and -C in HEK293 Cells

To evaluate functional differences between OATP-B and -C, uptakes of [^{3}H]estrone-3-sulfate and [^{3}H]estradiol-17β-glucironide were measured. First of all, the expression of both the OATP-B and -C in HEK293 cells by transient transfection using the calcium phosphate precipitation method was confirmed by RT-PCR. As clearly shown in Fig. 1, each corresponding PCR-product for OATP-B and -C was detected only when the RNA extracted from the HEK293 cells transfected either cDNA of OATP-B or -C was used for RT template. Uptakes of both compounds by HEK293 cells transfected with either OATP-B or -C were compared with those by vector-transfected (mock) cells as shown in Fig. 2. [^{3}H]Estrone-3-sulfate showed significantly increased uptake by both of OATP-B and -C-transfected cells compared with that by mock-transfected cells (Fig. 2a). However, although [^{3}H]es-

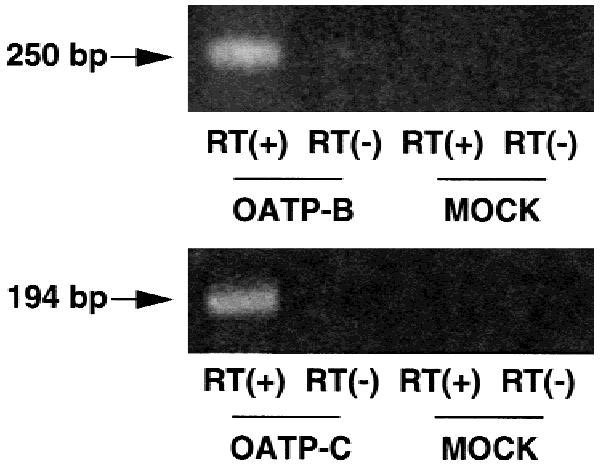

Fig. 1. Expression of OATP-B and OATP-C in transiently transfected HEK293 cells. RT-PCR was performed using RNA obtained from the cells transfected with OATP-B- or OATP-C-cDNA. The reaction was performed as described in Materials and Methods. Specific bands corresponding to OATP-B and -C are shown by arrows with sizes of 250 and 194 bps, respectively. RT(+) and RT(−) represent the PCR with and without previous RT reactions, respectively.

tradiol-17β-glucuronide was taken up by OATP-C, its uptake by OATP-B was negligible (Fig. 2b). Based on these results, uptake kinetics of estrone-3-sulfate by OATP-B and -C and estradiol-17β-glucuronide by OATP-C were analyzed at 30 min, which exhibited significantly and reliably increased uptake by transfecting cDNAs and before attained steady state, by means of Eadie–Hofstee plots. Figure 3a–c shows the uptakes of estrone-3-sulfate by OATP-B and -C and the uptake of estradiol-17β-glucuronide by OATP-C, respectively. Uptakes of estrone-3-sulfate by OATP-B and estradiol-17β-glucuronide by OATP-C gave linear plots, whereas uptake of estrone-3-sulfate was apparently biphasic, suggesting the presence of two kinetically distinct functional sites on OATP-C. The obtained half-saturation concentration (K_m) and maximum uptake rate (V_{max}) of estrone-3-sulfate by OATP-B were 9.04 ± 3.17 μM and 531 ± 92.7 pmol/mg protein/30 min, respectively. In the case of OATP-C, K_m and V_{max} for estradiol-17β-glucuronide were 3.71 ± 0.34 μM and 128 ± 3.97 pmol/mg protein/30 min, respectively, and the values for the high- and low-affinity components of estrone-3-sulfate uptake were 67.5 ± 31.6 nM and 7.00 ± 2.17 μM (K_m) and 14.8 ± 4.12 pmol/mg protein/30 min and 549 ± 119 pmol/mg protein/30 min (V_{max}), respectively.

Characteristics of Transport of Estrone-3-Sulfate by OATP-C Expressed in *Xenopus* Oocytes

Because unusual biphasic kinetics in OATP-C-mediated transport of estrone-3-sulfate was observed using HEK293 cells as shown in Fig. 3C, the characteristics was confirmed by using different transporter expression system, *Xenopus* oocytes. Uptake of [^{3}H]estrone-3-sulfate by oocytes expressed with OATP-C was significantly higher than that by water-injected oocytes (Fig. 4a). When concentration dependence of the uptake of estrone-3-sulafate by OATP-C was evaluated, Eadie–Hofstee plot analysis showed biphasic kinetics (Fig. 4b). The values for the high- and low-affinity components of estrone-3-sulfate uptake were 94.0 ± 53.0 nM and 5.34 ± 5.70 μM (K_m) and 0.151 ± 0.065 pmol/oocyte/30 min and 0.751 ± 0.329 pmol/oocyte/30 min (V_{max}), respectively. These transport characteristics are very similar with those of observed in HEK293 cells.

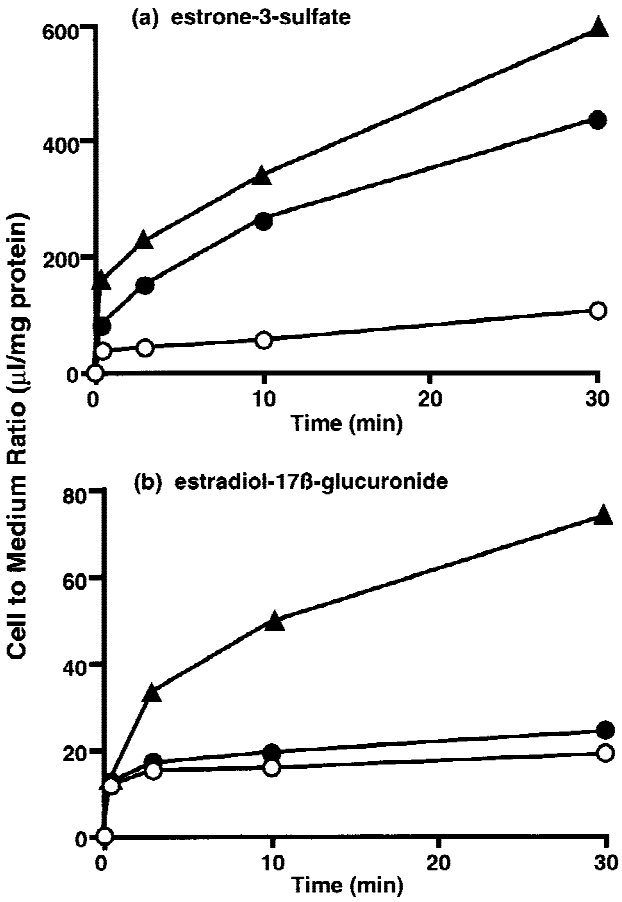

Fig. 2. Time courses for the uptakes of estrone-3-sulfate (a) and estradiol-17-β-glucuronide (b) by OATP-B or OATP-C. Uptakes of (a) [^{3}H]estrone-3-sulfate (4.8 nM) and (b) [^{3}H]estradiol-17β-glucuronide (5.7 nM) were measured over 30 min using HEK293 cells transfected with pcDNA vector alone (○), or vector containing OATP-B (●) or OATP-C cDNA (▲). The uptake was expressed as cell-to-medium ratio, which was obtained by dividing the amount taken up in the cells by the substrate concentration in the uptake medium. Each result is the mean ± SEM (n = 3 or 4). When error bars are not shown, they are smaller than symbols.

Mutual Inhibitory Effects on Uptakes of Estradiol-3-Sulfate and Estradiol-17β-Glucuronide by OATP-C

Because estrone-3-sulfate and estradiol-17β-glucuronide had different numbers of functional sites on OATP-C, the identity of the binding sites was examined by studying the mutual inhibition kinetics in HEK293 cells. Figure 5, a and b shows the Eadie–Hofstee plots of uptakes of estradiol-17β-glucuronide and estrone-3-sulfate, respectively, in the presence or absence of an inhibitor. By the addition of 50 nM estrone-3-sulfate, the apparent K_m of estradiol-17β-glucuronide was increased to 7.75 ± 1.09 μM from 3.71 μM without significant change in apparent V_{max} (124 ± 6.97 pmol/mg protein/30 min from 128 pmol/mg protein/30 min). Based on the competitive inhibition kinetics, the K_i value of estrone-3-sulfate for the uptake of estradiol-17β-glucuronide was 45.8

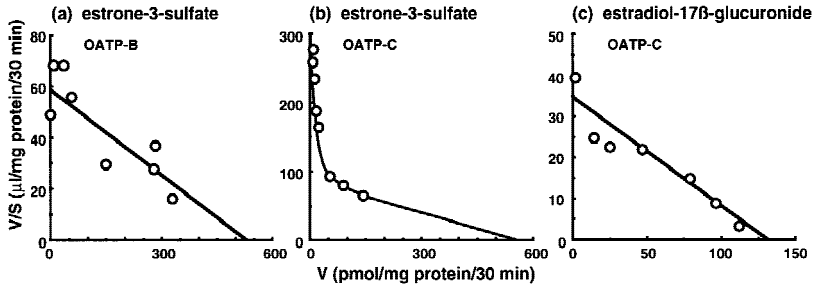

Fig. 3. Eadie–Hofstee plots of uptakes of estrone-3-sulfate and estradiol-17β-glucuronide by OATP-B or OATP-C. Uptakes of estrone-3-sulfate by OATP-B (a) and by OATP-C (b) and estradiol-17β-glucuronide by OATP-C (c) at various concentrations were measured for 30 min. Specific uptake was evaluated by subtracting uptake by mock cells from total uptake by OATP-B or -C-transfected cells. Lines represent the calculated values using the kinetic parameters obtained by nonlinear least-squares analysis. Each point is mean value (n = 3 or 4).

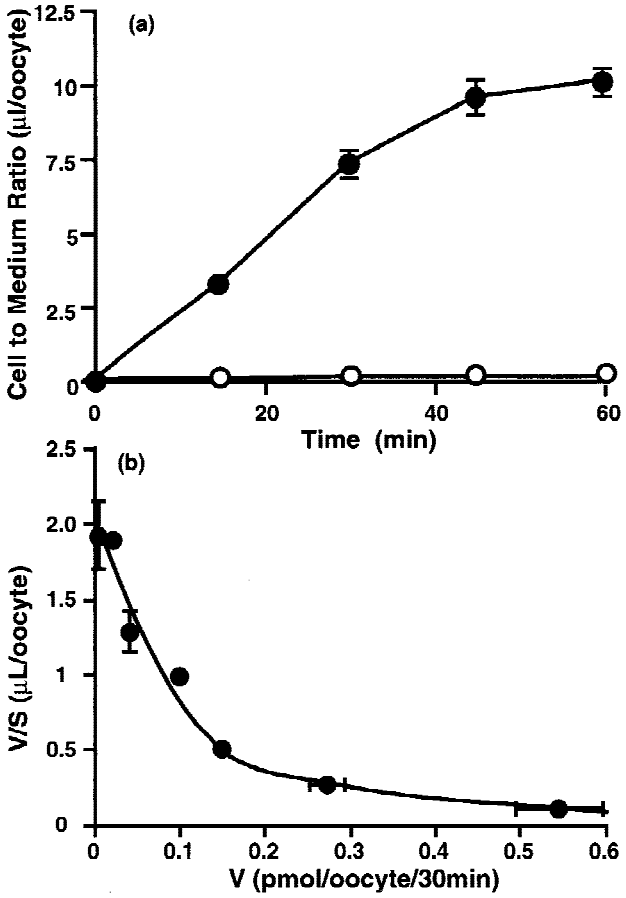

Fig. 4. Time course and Eadie–Hofstee plot of uptakes of estrone-3-sulfate by *Xenopus* oocytes injected with cRNA of OATP-C. (a) Uptake of [^{3}H]estrone-3-sulfate (3.6 nM) was measured at 25°C. ○ and ● represent the results in water- and OATP-C cDNA-injected oocytes, respectively. (b) Uptake of estrone-3-sulfate at various concentrations from 10 nM to 10 µM was measured for 30 min at 25°C, and the uptake is shown by Eadie–Hofstee plot after subtraction of the uptake by water-injected oocytes. Solid line represents the calculated values using the kinetic parameters obtained by nonlinear least-squares analysis. Each point is mean ± SEM (n = 5 to 8 oocytes).

± 15.2 nM. The addition of 8 µM estradiol-17β-glucuronide decreased uptake of estrone-3-sulfate at the high-affinity site without significant change of low-affinity component (Fig. 3b). In this case, the intercept on the y-axis was decreased, so, the inhibition kinetics was analyzed by assuming competitive inhibition of estrone-3-sulfate uptake by estradiol-17β-glucuronide only at the high-affinity site. The apparent K_m and V_{max} of the high-affinity site in the presence of estradiol-17β-glucuronide were 190 ± 87.7 nM and 18.5 ± 2.90 pmol/mg protein/30 min, respectively, revealing a significant change from the control in K_m alone (Fig. 3b). The evaluated K_i value of estradiol-17β-glucuronide was 4.43 ± 1.96 µM. The K_i (45.8 nM) and K_m (67.5 nM) of the high-affinity component for estrone-3-sulfate were comparable. Similarly, K_m (3.71 µM) and K_i (4.43 µM) of estradiol-17β-glucuronide were almost identical. These results demonstrated that only the high-affinity site of estrone-3-sulfate transport is shared with estradiol-17β-glucuronide on OATP-C, and the low-affinity site for estrone-3-sulfate on OATP-C hardly accepts estradiol-17β-glucuronide as a substrate.

Substrate Specificity of OATP-B and -C

The difference of substrate specificity between OATP-B and -C was studied by examining inhibitory effects on the uptake of a common substrate, [^{3}H]estrone-3-sulfate, at a low concentration 4 nM, to focus on the high-affinity component. Figures 6 and 7 show the inhibitory effects on the uptake of [^{3}H]estrone-3-sulfate of various conjugated metabolites of estradiol and estrone, respectively. Inhibitory effects of conjugated metabolites of estradiol on the uptakes of [^{3}H]estrone-3-sulfate by OATP-B and -C are shown in Fig. 6, a and b, respectively. In the case of OATP-C, all of the inhibitors examined, including unconjugated estradiol, estradiol-17β-glucuronide, estradiol-3-sulfate, and estradiol-17β-glucuronide-3-sulfate, significantly reduced the uptake of [^{3}H]estrone-3-sulfate, although the minimum effective concentrations ranged from 1 µM to 10 µM. By contrast, in the case of OATP-B only a high concentration (100 µM) of unconjugated estradiol or estradiol-3-sulfate showed significant reduction of the uptake of [^{3}H]estrone-3-sulfate, while glucuronide conjugates were not inhibitory. When estrone and its conjugated metabolites such as estrone-3-glucuronide and estrone-3-sulfate were used as inhibitors, OATP-C-mediated

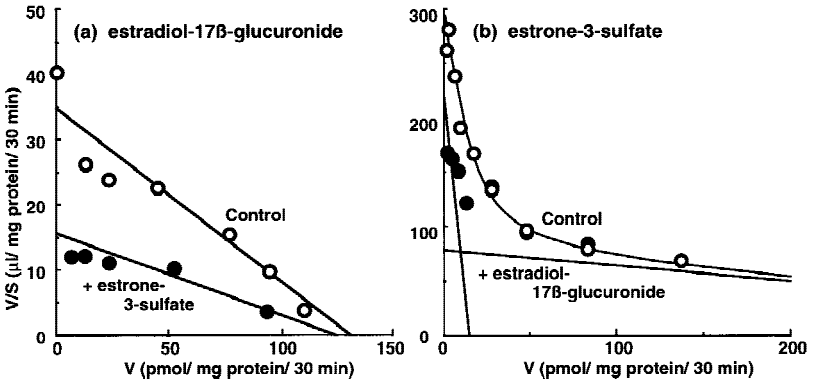

Fig. 5. Eadie–Hofstee plots of mutual inhibitory effects on uptakes of estradiol-17β-glucuronide (a) and estrone-3-sulfate (b) by OATP-C. Uptake was measured for 30 min at 37°C in the presence (●) or absence of inhibitors (○). Inhibitor concentrations of estrone-3-sulfate and estradiol-17β-glucuronide were 50 nM (a) and 8 μM (b), respectively. The solid lines were generated by the kinetic parameters obtained as described in the text.

uptake of [^{3}H]estrone-3-sulfate was inhibited by both of the conjugated metabolites at 1 μM and by the unconjugated compound at 100 μM, as shown in Fig. 7b. In the case of OATP-B (Fig. 7a), estrone-3-glucuronide did not inhibit the uptake of [^{3}H]estrone-3-sulfate at 100 μM but apparently increased it at 1 μM. Sulfate conjugate of and unconjugate of estrone showed significant inhibition at 10 and 100 μM, respectively. Although the observed inhibitory potencies do not necessarily identify the substrates of the inhibited transporter, the results demonstrated a difference in the substrate selectivity of the two transporters, OATP-B and -C. OATP-C-mediated uptake of [^{3}H]estrone-3-sulfate was reduced by various steroid conjugates, and few of the compounds showed any inhibitory effect on the uptake by OATP-B. The estrone conjugated with sulfate at the 3-position showed a stronger inhibitory effect than did the glucuronidated form, for both OATP-B and -C. Although 100 μM estradiol-17β-glucuronide apparently showed stronger inhibitory effect on OATP-C-mediated uptake of [^{3}H]estrone-3-sulfate than that by estradiol-3-sulafte (Fig. 6b), more specific inhibitory effect observed at lower concentrations 1 and 10 μM showed that β-glucuronidation at the 17-position of estradiol decreased the inhibitory potencies for both OATP-B and -C, suggesting that 17β-glucuronidation is unfavorable for recognition by the transporters.

DISCUSSION

In the present study, the functional properties of OATP-B were compared with those of OATP-C, an important transporter in the hepatic uptake/elimination of various organic anions and conjugated metabolites (8,10–13,20). Although [^{3}H]estrone-3-sulfate was transported by both OATP-B and -C, another conjugated steroid, [^{3}H]estradiol-17β-glucuronide, was transported only by OATP-C. Accordingly, OATP-B and -C have differential substrate specificities

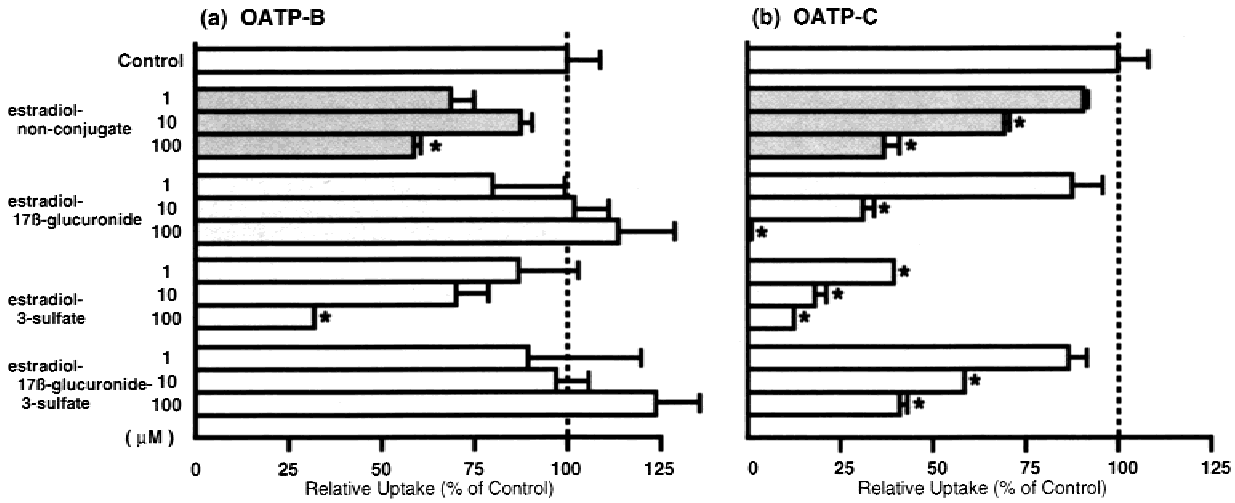

Fig. 6. The inhibitory effects of unconjugated or conjugated estradiol on the uptakes of [^{3}H]estrone-3-sulfate by OATP-B (a) and OATP-C (b). Uptake of [^{3}H]estrone-3-sulfate (4 nM) was measured for 30 min and the results are shown as a percentage of control uptake measured in the absence of inhibitor after correcting for the uptake by the vector-transfected (mock) cells. The concentrations used for inhibition are indicated by the numbers in the figures. Each result is the mean and SEM (n = 3 or 4) and (*) indicates a significant difference from the control (P <0.05).

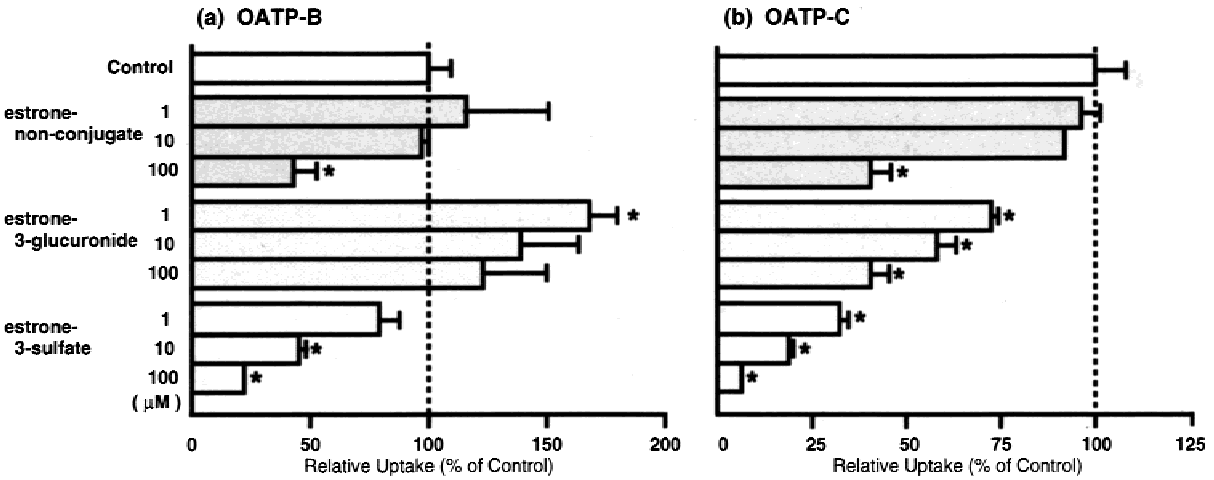

Fig. 7. The inhibitory effects of unconjugated or conjugated estrone on the uptakes of [^{3}H]estrone-3-sulfate by OATP-B (a) and OATP-C (b). Uptake of [^{3}H]estrone-3-sulfate (4 nM) was measured for 30 min and the results are shown as a percentage of control uptake measured in the absence of inhibitor after correcting for the uptake by vector-transfected (mock) cells. The concentrations used for inhibition are indicated by the numbers in the figures. Each result is the mean and SEM (n = 3 or 4) and (*) indicates a significant difference from the control (P <0.05).

and estrone-3-sulfate can be used as a model substrate, because it is commonly accepted as a substrate by both transporters.

To characterize further the functional properties, the affinities of the two conjugated steroids to the OATP-B and -C transporters were compared. Eadie–Hofstee plots of uptakes of estrone-3-sulfate by OATP-B and estradiol-17β-glucuronide by OATP-C each exhibited a single straight line with K_m values of 9.04 μM and 3.71 μM, respectively, in HEK293 cells. By contrast, OATP-C-mediated transport of estrone-3-sulfate was biphasic with high-affinity, low-capacity and low-affinity, high-capacity components having K_m of 67.5 nM and 7.0 μM and V_{max} of 14.8 and 549 pmol/mg protein/30 min, respectively, in HEK293 cells. Similarly, in *Xenopus* oocytes OATP-C-mediated transport of estrone-3-sulfate was biphasic with K_m values 94 nM and 5.34 μM. Because the obtained K_m values in HEK293 cells and *Xenopus* oocytes were comparable, the observation of biphasic transport of estrone-3-sulfate via OATP-C was confirmed to be specific and to be independent of experimental methods. Cui *et al.* examined estrone-3-sulfate transport by OATP-C using the same expression system (20), and their K_m (8.2 μM) is close to that of the low-affinity component obtained in the present studies (7.0 and 5.34 μM). The high-affinity component observed in the present study may be easily saturated and would be difficult to identify if the minimum concentration used for the kinetic study is not properly selected. In the present study, the specific OATP-C-mediated uptake was evaluated by subtracting the uptake by mock cells (transfected with expression vector alone) or water-injected oocytes from the total uptake, so the results should not be influenced by the native activity of HEK293 cells or oocytes. It is generally atypical that a single transporter molecule has two different functional sites. Several mechanisms can be considered to explain this observation; firstly, two sites may independently exhibit transport activity; secondly, substrate-binding to a low-affinity site may influence the functional high-affinity site so that the apparent affinity is lowered in the presence of higher concentrations of substrate; and thirdly, multiple conformations of the transporter protein may be formed when heterologous protein is abundantly expressed after gene-transfection, resulting in distinct states of the functional site (e.g., having different-sized binding pocket). Similar multiple affinity sites have been reported in the case of the drug-metabolizing cytochrome P-450 enzymes (21,22). Although in our case the precise mechanism of the apparent biphasic saturation kinetics is not yet clear, OATP-B seems to have a distinct substrate binding site from OATP-C, because OATP-B exhibited a single functional site for estrone-3-sulfate and negligible transport activity for estradiol-17β-glucuronide.

Mutual inhibition between estrone-3-sulfate and estradiol-17β-glucuronide for OATP-C-mediated transport could be explained by competitive inhibition, whereas such a study was impossible with OATP-B, because of the lack of the transport activity for estradiol-17β-glucuronide by OATP-B. The inhibition constant K_i of estrone-3-sulfate (45.8 nM) for OATP-C-mediated transport of estradiol-17β-glucuronide was comparable with the K_m of estrone-3-sulfate at the high-affinity site (67.5 nM). Similarly, K_i of estradiol-17β-glucuronide (4.43 μM) for OATP-C-mediated transport of estrone-3-sulfate was close to the K_m (3.71 μM), supposing that competition occurred only at the high-affinity site. Accordingly, the two steroid conjugates appear to share a common binding site on OATP-C, which corresponds to the high-affinity site for estrone-3-sulfate. The K_m value of estrone-3-sulfate for OATP-B (9.04 μM) was close to the low-affinity site of OATP-C. Because OATP-B cannot transport estradiol-17β-glucuronide and the low-affinity site for estrone-3-sulfate transport on OATP-C was not subject to competition from estradiol-17β-glucuronide, the functional site on OATP-B might have a similar milieu to the low-affinity site on OATP-C. Serum levels of estrone-3-sulfate fluctuate but are in the range of 1 to 10 nM in female (23). Therefore, the high-affinity component of OATP-C for estrone-3-sulfate may be physiologically more relevant than the low-affinity component.

Inhibition studies on the transport of [^{3}H]estrone-3-

sulfate by OATP-B and -C (Figs. 6 and 7) also demonstrated distinct substrate specificities between the two transporters. OATP-B-mediated transport of [^{3}H]estrone-3-sulfate was inhibited by sulfate conjugates of both estradiol and estrone, whereas glucuronidated steroids had little effect. In contrast, all conjugated steroids examined reduced the uptake of [^{3}H]estrone-3-sulfate by OATP-C. A double conjugate, estradiol-17β-glucuronide-3-sulfate did not change the uptake of [^{3}H]estrone-3-sulfate by OATP-B, whereas it inhibited the uptake by OATP-C. Furthermore, unconjugated forms of estradiol and estrone reduced the transport activity of both OATP-B and -C at high concentration, 10 or 100 μM. However, glucuronide conjugates failed to inhibit OATP-B even at a concentration as high as 100 μM. These inhibition profiles and the absence of transport activity of [^{3}H]estradiol-17β-glucuronide by OATP-B clearly show that glucuronidation is unfavorable for transport by OATP-B. So, OATP-B and -C have quite distinct affinities for glucuronide conjugates. The strong inhibitory potencies of sulfate conjugates on [^{3}H]estrone-3-sulfate uptake by both OATP-B and -C suggests that anionic charge is essential but smaller molecular size may be more favorable for binding to both OATP-B and -C. Interestingly, lower concentration of estrone-3-glucuronide (1 μM) apparently increased the uptake of [^{3}H]estrone-3-sulfate by OATP-B and the extent of the increase was disappeared at higher concentrations of estrone-3-glucuronide (10 and 100 μM) (Fig. 7a). Although the reason for such increase is not clear at present, similarly increased uptake of estradiol-17β-glucuronide via organic anion transporter MRP3 was observed in the presence of sulfate conjugates of E3040 and 4-methylumbelliferone (24). Further studies such as bidirectionality and driving forces for OATP transporters will be essential to clarify the underlying mechanisms.

OATP-A transported both estradiol-17β-glucuronide and estrone-3-sulfate, like OATP-C, though the transport activity for the glucuronide conjugate was relatively weak (25). OATP-8 transported estradiol-17β-glucuronide, but showed no detectable transport activity for estrone-3-sulfate (20). Therefore, human OATPs might be classified in terms of their affinities for different steroid conjugates. Similar differences of affinities for glucuronide and sulfate conjugates have been found in other anion transporters. In the case of the organic anion transporter OAT4, which is expressed in placenta and kidney and transports organic anions, including estrone-3-sulfate, similar inhibitory effects were observed (26). Various sulfate conjugates reduced the OAT4-mediated uptake of [^{3}H]estrone-3-sulfate, but the corresponding β-glucuronide conjugates did not. Differential effects of glucuronidated and sulfated metabolites on transport of [^{3}H]estradiol-17β-glucuronide were also reported for MRP3, although in this case glucuronide conjugates exhibited stronger inhibitory effects than sulfate conjugates (24). After submission of the present study, Kullak–Ublick reported the functional differences among four human OATPs, OATP-A, OATP-B, OATP-C, and OATP-8 and found the same result with the present study that OATP-B transports estrone-3-sulfate but not estradiol-17β-glucuronide (27). Their results also suggested that OATP-B has restricted substrate specificity compared with OATP-C that shows broader substrate specifity, although the difference of affinity between these two transporters to the present steroid conjugates is not clearly shown.

A preliminary study has shown that dehydroepiandrosterone sulfate, a substrate of OATP-C, was also transported by OATP-B (data not shown). In addition, the hydroxymethylglutaryl-coenzyme A reductase inhibitor pravastatin, which is also a substrate of OATP-C (13) was weakly but significantly taken up by HEK293 cells transfected with OATP-B (data not shown). Similarly, the antibiotic benzylpenicillin was also weakly transported by OATP-B (12). Accordingly, OATP-B is presumed to accept sulfated steroids well and also to transport other anionic drugs with relatively low activity.

Identification of the counterpart of OATP-B in animals such as rats is important to characterize further the physiological roles of OATP-B *in vivo*. The recently found rat transporter moat1 showed high amino acid sequence similarity with OATP-B, transported prostaglandins and leukotriene C_4 and is distributed in various tissues (17). However, dehydroepiandrosterone sulfate was not transported by moat1 and this transporter is expressed in brain, whereas OATP-B is negligibly expressed in brain (12) and showed transport activity for dehydroepiandrosterone sulfate. Rat lst1 and rat oatp1 and 2 have shown highly specific tissue distributions in liver, kidney and/or brain and they transport both sulfated and glucuronidated steroids (14–16,28). Tissue expression of rat oatp3 is rather broad in kidney, retina, brain, lung and small intestine (15,29), being similar to that of OATP-B (12). However, the substrate specificities are not identical and the structural homology between oatp3 and OATP-B proteins is not high (about 30%). Accordingly, the rat oatp molecule corresponding to human OATP-B is not clear. In addition, the physiologic substrates/roles of OATP-B are not yet clearly understood, and clarification of these points will facilitate the identification of the counterpart of OATP-B in animals.

In conclusion, in the present study it was clearly demonstrated that OATP-B preferentially transports sulfate conjugates of steroids, but cannot accept glucuronide conjugates as substrates. The absence of affinity for glucuronide conjugates distinguishes OATP-B from OATP-C, and may be unique among known human OATPs. Furthermore, kinetic study of OATP-C-mediated transport of estrone-3-sulfate revealed that two functional sites were apparently involved, with high and low affinities. Estradiol-17β-glucuronide and estrone-3-sulfate shared only the high-affinity functional site. This is the first demonstration of two apparent functional sites on a single OATP transporter, and the K_m of the high-affinity site may be physiologically relevant. Such precise functional studies are needed to provide the required information to characterize each OATP transporter in human and to identify the counterpart transporters in animals.

ACKNOWLEDGMENTS

We thank Chisato Tsukada for her excellent technical assistance. This work was supported in part by a grant-in-aid for Scientific Research from the Ministry of Education, Science, Sports, and Culture, Japan, and a grant from the Japan Health Sciences Foundation Drug Innovation Project.

REFERENCES

1. M. Müller and P. L. M. Jansen. Molecular aspects of hepatobiliary transport. *Am. J. Physiol.* **272**:G1285–G1303 (1997).
2. T. Sekine, S.H. Cha, and H. Endou. The multispecific organic

anion transporter (OAT) family. *Pflügers Arch*. **440**:337–350 (2000).
3. H. Yabuuchi, I. Tamai, K. Morita, T. Kouda, K. Miyamoto, E. Takeda, and A. Tsuji. Hepatic sinusoidal membrane transport of anionic drugs mediated by anion transporter *Npt*1. *J. Pharmacol. Exp. Ther*. **286**:1391–1396 (1998).
4. H. Uchino, I. Tamai, K. Yamashita, Y. Minemoto, Y. Sai, H. Yabuuchi, K. Miyamoto, E. Takeda, and A. Tsuji. *p*-Aminohippuric acid transport at renal apical membrane mediated by human inorganic phosphate transporter NPT1. *Biochem. Biophys. Res. Commun*. **270**:254–259 (2000).
5. E. Jacquemin, B. Hagenbuch, B. Stieger, A. W. Wolkoff, and P. J. Meier. Expression cloning of a rat liver Na^+-independent organic anion transporter. *Proc. Natl. Acad. Sci. USA* **91**:133–137 (1994).
6. A. J. Bergwerk, X. Shi, A. C. Ford, N. Kanai, E. Jacquemin, R. D. Burk, S. Bai, P. M. Novikoff, B. Stieger, P. J. Meier, V. L. Schuster, and A. W. Wolkoff. Immunologic distribution of an organic anion transport protein in rat liver and kidney. *Am. J. Physiol*. **271**:G231–G238 (1996).
7. R. Lu, N. Kanai, Y. Bao, and V. L. Schuster. Cloning, in vitro expression, and tissue distribution of a human prostaglandin transporter cDNA (hPGT). *J. Clin. Invest*. **98**:1142–1149 (1996).
8. T. Abe, M. Kakyo, T. Tokui, R. Nakagomi, T. Nishio, D. Nakai, H. Nomura, M. Unno, M. Suzuki, T. Naitoh, S. Matsuo, and H. Yawo. Identification of a novel gene family encoding human liver-specific organic anion transporter LST-1. *J. Biol. Chem*. **274**: 17159–17163 (1999).
9. G. A. Kullak-Ublick, B. Hagenbush, B. Stieger, C. D. Schteingart, A. F. Hoffman, A. W. Wolkoff, and P. J. Meier. Molecular and functional characterization of an organic anion transporting polypeptide cloned from human liver. *Gastroenterology* **109**: 1274–1282 (1995).
10. J. Konig, Y. Cui, A. T. Nies, and D. Keppler. Localization and genomic organization of a new hepatocellular organic anion transporting polypeptide. *J. Biol. Chem*. **275**:23161–23168 (2000).
11. J, Konig, Y. Cui, A. T. Nies, and D. Keppler. A novel human organic anion transporting polypeptide localized to the basolateral hepatocyte membrane. *Am. J. Physiol*. **278**:G156–G164 (2000).
12. I. Tamai, J. Nezu, H. Uchino, Y. Sai, A. Oku, M. Shimane, and A. Tsuji. Molecular identification and characterization of novel members of the human organic anion transporter (OATP) family. *Biochem. Biophys. Res. Commun*. **273**:251–260 (2000).
13. B. Hsiang, Y. Zhu, Z. Wang, Y. Wu, V. Sasseville, W.-P. Yang, and T. G. Kirchgessner. A novel human hepatic organic anion transporting polypeptide (OATP-2). *J. Biol. Chem*. **274**:37161–37168 (1999).
14. B. Noé, B. Hagenbuch, B. Stieger, and P. J. Meier. Isolation of a multispecific organic anion and cardiac glycoside transporter from rat brain. *Proc. Natl. Acad. Sci. USA* **94**:10346–10350 (1997).
15. T. Abe, M. Kakyo, H. Sakagami, T. Tokui, T. Nishio, M. Tanemoto, H. Nomura, S. C. Hebert, S. Matsuno, H. Kondo, and H. Yawo. Molecular characterization and tissue distribution of a new organic anion transporter subtype (oatp3) that transports thyroid hormones and taurocholate and comparison with oatp2. *J. Biol. Chem*. **273**:22395–22401 (1998).
16. V. Cattori, B. Hagenbuch, N. Hagenbuch, B. Stieger, R. Ha, K. E. Winterhalter, and P. J. Meier. Identification of organic anion transporting polypeptide 4 (Oatp4) as a major full-length isoform of the liver-specific transporter-1 (rlst-1) in rat liver. *FEBS Lett*. **474**:242–245 (2000).
17. T. Nishio, H. Adachi, R. Nakagomi, T. Tokui, E. Sato, M. Tanemoto, K. Fujiwara, M. Okabe, T. Onogawa, T. Suzuki, D. Nakai, K. Shiiba, M. Suzuki, H. Ohtani, Y. Kondo, M. Unno, S. Ito, K. Iinuma, K. Nunoki, S. Matsuno, and T. Abe. Molecular identification of a rat novel organic anion transporter moat1, which transports prostaglandin D(2), leukotriene C(4), and taurocholate. *Biochem. Biophys. Res. Commun*. **275**:831–838 (2000).
18. P. V. Balimane, I. Tamai, A. Guo, T. akanishi, H. Kitada, F. H. Leibach, A. Tsuji, and P. J. Sinko. Direct evidence for peptide transporter (PepT1)-mediated uptake of a nonpeptide prodrug, valacyclovir. *Biochem. Biophys. Res. Commun.* **250**:246–251 (1998).
19. M. M. Bradford. A rapid and sensitive method for the quantitation of microgram quantities of protein utilizing the principle of protein-dye binding. *Anal. Biochem.* **72**:248–254 (1976).
20. Y. Cui, J. Konig, I. Inka, U. Buchholz, and D. Keppler. Hepatic uptake of bilirubin and its conjugates by the human organic anion-transporting poly peptide SLC21A6. *J. Biol. Chem.* **276**: 9626–9630 (2001).
21. T. Iwatsubo, H. Suzuki, N. Shimada, K. Chiba, T. Ishizaki, C. E. Green, C. A. Tyson, T. Yokoi, T. Kamataki, and Y. Sugiyama. Prediction of in vivo hepatic metabolic clearance of YM796 from in vitro data by use of human liver microsome and recombinant P-450 isozymes. *J. Pharmacol. Exp. Ther*. **282**:909–919 (1997).
22. K. R. Korzekwa, N. Krishnamachary, M. Shou, A. Ogai, R. A. Parise, A. E. Rettie, F. J. Gonzalez, and T. S. Tracy. Evaluation of atypical cytochrome P450 kinetics with two-substrate model: Evidence that multiple substrates can simultaneously bind to cytochrome P450 active sites. *Biochemistry* **37**:4137–4147 (1998).
23. H. Honjo, J. Kitawaki, M. Itoh, J. Yasuda, K. Iwasaku, M. Urabe, K. Naitoh, T. Yamamoto, H. Okada, T. Ohkubo, and T. Nambara. Serum and urinary estrone sulfate during the menstrual cycle, measured by a direct radioimmunoassay, and fate of exogenously injected estrone sulfate. *Hormone Res*. **27**:61–68 (1987).
24. T. Hirohashi, H. Suzuki, and Y. Sugiyama. Characterization of the transport properties of cloned rat multidrug resistance-associated protein 3 (MRP3). *J. Biol. Chem*. **274**:15181–15185 (1999).
25. P. J. Meier, U. Eckhardt, A. Schroeder, B. Hagenbuch, and B. Stieger. Substrate specificity of sinusoidal bile acid and organic anion uptake systems in rat and human liver. *Hepatology* **26**: 1667–1677 (1997).
26. S. H. Cha, T. Sekine, H. Kusuhara, E. Yu, J. Y. Kim, D. K. Kim, Y. Sugiyama, Y. Kanai, and H. Endou. Molecular cloning and characterization of multispecific organic anion transporter 4 expressed in the placenta. *J. Biol. Chem.* **275**:4507–4512 (2000).
27. G. A. Kullak-Ublick, M. G. Ismair, S B. tieger, L. Landmann, R. Huber, F. Pizzagalli, K. Fattinger, P. J. Meier, and B. Hagenbuch. Organic anion-transporting polypeptide B (OATP-B) and its functional comparison with three other OATPs of human liver. *Gastroenterology* **120**:525–533 (2001).
28. M. Kakyo, H. Sakagami, T. Nishio, D. Nakai, R. Nakagomi, T. Tokui, T. Naitoh, S. Matsuno, T. Abe, and H. Yawo. Immunohistochemical distribution and functional characterization of an organic anion transporting polypeptide 2 (oatp2). *FEBS Lett*. **445**: 343–346 (1999).
29. H. C. Walters, A. L. Craddock, H. Fusegawa, M. C. Willingham, and P. A. Dawson. Expression, transport properties, and chromosomal location of organic anion transporter subtype 3. *Am. J. Physiol*. **279**:G1188–G1200 (2000).